Laser-induced fluorescence from the $E1$ and $F1$ states of the HgZn excimer

E. Hegazi, J. Supronowicz, G. Chambaud,* J. B. Atkinson, W. E. Baylis, and L. Krause

Department of Physics, University of Windsor, Windsor, Ontario, Canada N9B 3P4
and Ontario Laser and Lightwave Research Centre, Windsor, Ontario, Canada N9B 3P4

Pump and probe methods of laser spectroscopy were used to excite fluorescence from the $E1$ and $F1$ states of the HgZn excimer. Several bound-free and bound-bound fluorescence bands as well as excitation bands were recorded and correlated with a potential-energy diagram that includes the various spin-orbit components and supersedes the previously published potential-energy diagram based on Hund's case-(a) coupling.

I. INTRODUCTION

We have recently reported a study of the fluorescence spectrum of HgZn in the 2380–2650-Å region, which we interpreted in terms of transitions between molecular states derived from a preliminary potential-energy (PE) diagram drawn according to Hund's case-(a) coupling.[1,2] We now report further previously unobserved excitation and fluorescence spectra which we recorded using "pump and probe" methods and which we interpret with the aid of a more realistic PE diagram drawn and labeled according to Hund's case-(c) coupling and based on theoretical estimates. There is reasonable correlation between the experimentally recorded spectra and the PE curves which are still to be regarded as preliminary.

II. POTENTIAL-ENERGY CURVES

As the result of progress in *ab initio* calculations of the HgZn PE curves for the 13 lowest states in Hund's case (a), some considerable modifications must be made in the previously published PE diagram.[2] The revisions are made on the basis of preliminary self-consistent-field–configuration-interaction (SCF-CI) calculations carried out at internuclear separations of 5, 6, 7, and 10 bohr and diagonalizations of the asymptotic spin-orbit operator. Most of the minima in the excited states occur in the vicinity of $R = 5$ bohr. Further work is underway to refine the calculation of both spin-orbit and correlation contributions. The revised PE diagram, according to Hunds' case-(a) coupling, is shown in Fig. 1. It may be seen that, in comparison with the previous version,[2] the $^1\Pi(\text{Hg}\,^1S + \text{Zn}\,^1P)$ curve is slightly higher than previously assumed and does not cross the $^3\Sigma(\text{Hg}\,^1S + \text{Zn}\,^3P)$ curve at $R > 4.5$ bohr; as a result, the $^1\Pi$ state cannot be efficiently populated through a curve crossing with the $^3\Sigma$ state. The $^3\Sigma$ and $^3\Pi$ states correlated with Hg ^3P + Zn ^1S and higher asymptotic states are found to lie considerably lower near $R = 5$ bohr, because of an unexpectedly large admixture of the ionic configuration Hg$^-(^2P)$ + Zn$^+(^2S)$.

The preliminary results of the calculations also provide information about the nature of the wave functions in the molecular region. Accordingly, the $^3\Pi$ and $^3\Sigma$ (Hg ^1S + Zn ^3P) states are roughly half-ionic

[Hg$^-(^2P)$ + Zn$^+(^2S)$] and half-covalent (Hg ^1S + Zn ^3P). Similarly, the $^1\Pi(\text{Hg}\,^1S + \text{Zn}\,^1P)$ state is also an approximately equal mix of ionic [Hg$^-(^2P)$ + Zn$^+(^2S)$] and covalent (Hg ^1S + Zn ^1P) parts, and the more highly excited states also contain a significant ionic character. Thus, the ionic states of the system (Hg$^-$ + Zn$^+$) and, to a lesser extent (Hg$^+$ + Zn$^-$), do not simply cross the covalent states at various R values,[2] but instead interact strongly with all the molecular states, at least in the molecular region.

Our knowledge of the approximate nature of the wave functions has allowed us to estimate the spin-orbit splittings between the molecular states near $R = 5$ bohr, and to produce a PE diagram in Hund's case (c), with noncrossing curves for like Ω values. Preliminary PE diagrams for $\Omega = 0^+$, 0^-, 1, and 2 are shown in Figs. 2–5, and are used subsequently to interpret the observed fluorescence and excitation spectra that arise from transitions subject to the selection rules $\Delta\Omega = 0, \pm 1, + \leftrightarrow +$, $- \leftrightarrow -$, $+ \nleftrightarrow -$.[3]
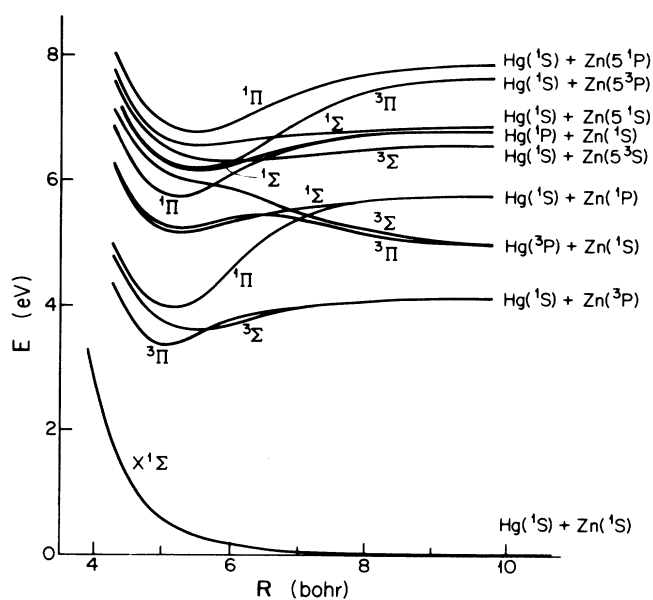

FIG. 1. PE diagram for HgZn, drawn and labeled according to Hund's case-(a) coupling.

FIG. 2. PE diagram according to Hund's case (c), showing states with $\Omega = 0^+$.
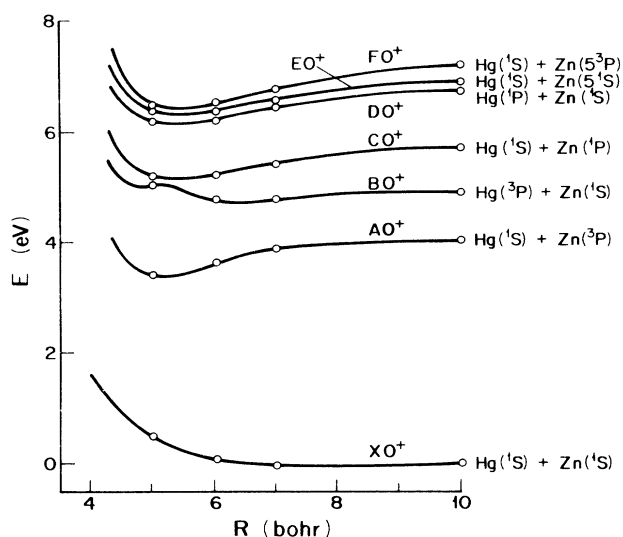

FIG. 4. PE diagram according to Hund's case (c), showing states with $\Omega = 1$.

III. EXPERIMENTAL DETAILS

The arrangement of the apparatus and the preparation of the HgZn vapor cell have been described previously.[1,4] The Hg-Zn vapor mixture contained in a quartz cell was irradiated with two collinear pulsed laser beams directed antiparallel to each other and timed to produce a 450-ns delay between the "pump" and "probe" pulses. The pump pulses consisted of 3075.9 Å radiation produced by frequency doubling the output of a two-stage dye laser (operated with Rh 640 in methanol), pumped with the second harmonic (5320 Å) of a Q-switched Nd:YAG (yttrium aluminum garnet) laser. Their purpose was to produce a population of the HgZn reservoir states $A0^-$, $A0^+$, and $A1$. The probe laser consisted of a second
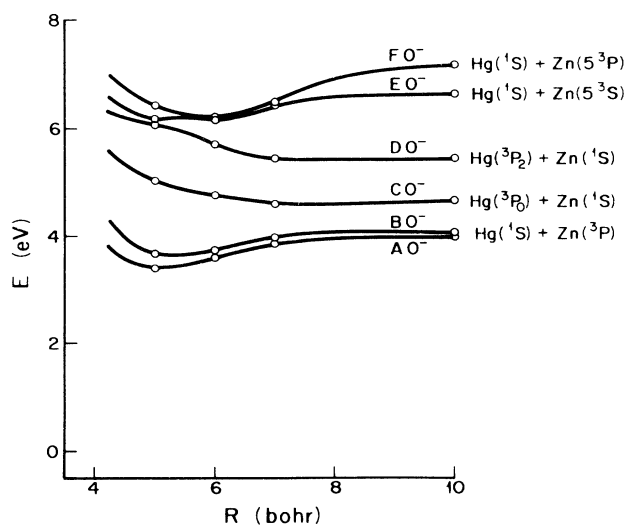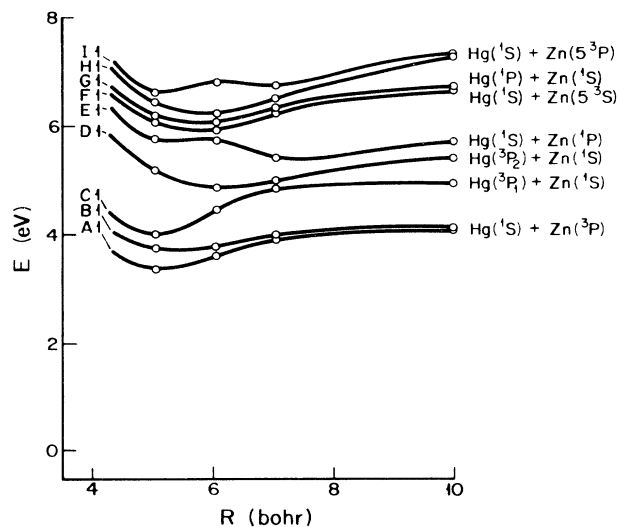
two-stage dye laser excited with a N_2 laser, and produced an output in the range 4000–4500 Å. The laser output wavelengths were measured with a precision of ± 1 Å using a Fizeau wavelength meter.[5] The resulting bound-free uv fluorescence, emitted at right angles to the laser beams, was dispersed by a monochromator (I.S.A., H-20) fitted with a 1200-line/mm holographic grating and detected by an EMI 9816QB photomultiplier, which had a maximal resolution of about 4 Å at 2000 Å. A second monochromator (I.S.A., HR-320) fitted with a 1800-line/mm grating and an RCA 31034A photomultiplier was used to register the bound-bound fluorescence spectra with a resolution of about 0.5 Å. The signal integrating and averaging system consisted of a Biomation Model 6500 transient digitizer which had a time resolution of 2

FIG. 3. PE diagram according to Hund's case (c), showing states with $\Omega = 0^-$.

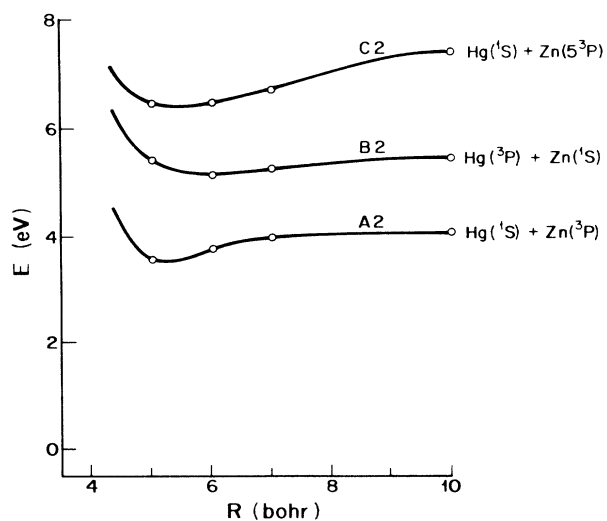FIG. 5. PE diagram according to Hund's case (c), showing states with $\Omega = 2$.

ns/channel and was controlled by a Commodore PET 2001 microcomputer. Two computer-controlled stepper motors were used to scan, in constant wavelength increments, the probe laser and the monochromator whose smallest scanning increments were $1/24$ and 0.5 Å, respectively.

The experiment consisted of two complementary parts. During the first part, the monochromator was scanned in steps of 2, 3, or 4 Å, while the probe laser was tuned to a particular wavelength at which a strong fluorescence signal was observed. The monochromator was scanned in the 2200–2700-Å spectral region to register the bound-free fluorescence spectra and in the 4250–4500-Å region to record the bound-bound spectra. Both monochromator slits were at their narrowest setting ($\frac{1}{8}$ mm) and a "boxcar" time-averaging method was used for data acquisition. In the second part of the experiment, the monochromator was set on a fixed wavelength corresponding to a peak in the fluorescence band, while the probe laser was scanned in the region 4000–4500 Å. Three dyes were used to cover this spectral region: C440 in ethanol, St 420 in methanol, and DPS in p-dioxane. When exciting bound-free fluorescence, several excitation spectra were recorded with the monochromator set at different wavelengths. Different excitation spectra indicated that more than one state was responsible for the bound-free fluorescence. When exciting bound-bound "resonance" fluorescence, two fluorescence bands were registered, arising from the decays of the $v'=0$ and 1 vibrational states. The probe laser was scanned in 1- or 2-Å steps and a "boxcar" time-averaging method was used, as before.

IV. EXCITATION AND DECAY OF THE $E1$ AND $F1$ STATES

The $E1(\mathrm{Hg}\,^1S+\mathrm{Zn}\,^1P)$ and the $F1(\mathrm{Hg}\,^1S+\mathrm{Zn}5\,^3S)$ states were populated using the pump and probe method. The pump pulse produced populations of the $A1$, $A0^+$, and $A0^-$ $(\mathrm{Hg}\,^1S+\mathrm{Zn}\,^3P)$ states which became reservoir states, since $A0^-$ is a metastable state, and $A0^+$ and $A1$ are very likely in thermal equilibrium with it. The absorption of the pulsed probe radiation in the range 4000–4500 Å resulted in the population of specific vibrational levels of the $E1$ and $F1$ states.

The $E1$ state was excited by transitions from both $A0^+$ and $A0^-$ states and the $F1$ state from only one lower state which we believe to be the $A0^+$ state. Both $E1$ and $F1$ states were found to decay to the $X0^+$ ground state by bound-free transitions, giving rise to Condon internal diffraction (CID) spectra, and we also observed an $F1 \rightarrow A0^+$ decay by a bound-bound transition resulting in the emission of a resonance fluorescence spectrum. Because the CID spectra were emitted simultaneously in the same spectral region near 2260 Å following excitation with a single probe wavelength, they overlapped and there was some difficulty with their identification and analysis. An additional complication arose from the presence of a third (unidentified) partially resolved bound-free fluorescence spectrum extending over the range 2300–2660 Å, which was also excited by probe radiation of wavelength 4000–4500 Å and whose overall

profile was typical of a decay of a high vibrational level.

The assignments of these particular molecular states as participating in the various emission and absorption processes are based not only on the calculated PE curves and selection rules, but also on numerous additional spectra whose analysis has now been completed and which are found to be entirely consistent with the interpretation presented here.[6]

V. RESULTS AND DISCUSSION

A. The fluorescence spectrum in the 2230–2320-Å region

1. The $E1 \rightarrow X0^+$ fluorescence spectrum

Traces of the fluorescence bands emitted in the bound-free $E1 \rightarrow X0^+$ decay of the $v'=1$ and 0 levels are shown in Figs. 6(a) and 6(b), respectively. Both levels were excited from the $v''=0$ level of the $A0^+$ state, using probe-laser wavelengths of 4394 and 4421 Å, respectively. The CID patterns corresponding to these bands are partly overlaid by an additional CID pattern which has a much smaller spacing between maxima, exhibits prominent peaks near 2340 Å, and extends to 2660 Å. This CID "background," which can be seen in Fig. 6, has not yet been analyzed and its origin is to be further investigated. The prominent peaks near 2340 and 2290 Å were found to be a constituent part of this spectrum. The CID background might be due to bound-continuum transitions
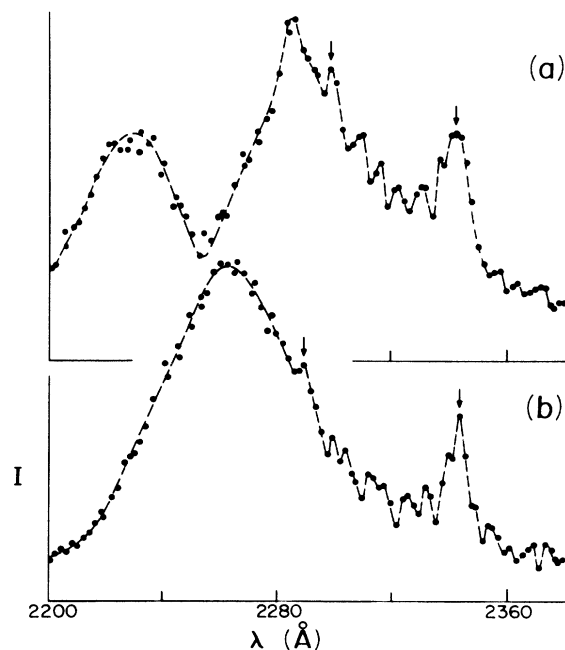

FIG. 6. Laser-induced fluorescence (LIF) bands emitted from selectively populated v' levels of the $E1$ state, excited from the $v''=0$, $A0^+$ state: (a) $v'=1$; (b) $v'=0$. The wavelengths of the probe radiation were (a) 4394 Å and (b) 4421 Å. The vertical arrows indicate peaks due to the "background" fluorescence spectrum.

from high vibrational levels of the CO^+ state, excited simultaneously with the $E1$ state, or from vibrational levels belonging to the second potential well of the $E1$ state, which could have been populated through the $E1\text{-}D0^-$ curve crossings through both $E1$ potential wells. It should be noted that the $E1$ state is quasibound with a barrier due to avoided crossings with $\Omega=1$ states correlated with $Hg(6\,^1P)+Zn(4\,^1S)$ and $Hg(6\,^1S)+Zn(5\,^3P)$. The quasibound levels appear bound for excitation purposes if the barrier is sufficiently opaque. As a result, the state is characterized by a small equilibrium internuclear separation (see Fig. 4) and the presence of only a few vibrational levels.

Using probe wavelengths longer than 4421 Å resulted in the excitation of the $E1$ $v'=0$ level from $A0^+$ $v''=1,2,3,4$ levels which were found to have an energy spacing of 194 ± 5 cm^{-1}. Using probe wavelengths shorter than 4421 Å resulted in the excitation of the $E1$ $v'=1,2,3$ levels from the $A0^+$ $v''=0$ state. For these levels the energy spacing was approximately 135 cm^{-1}, which corresponds to the vibrational frequency ω_e of the $E1$ state.

Figure 7 shows traces of the fluorescence bands emitted in the $E1\rightarrow X0^+$ decays of the $v'=1$ and 0 states which, in this case, were excited from the $A0^-$ $v''=0$ state by 4347- and 4372-Å probe radiation, respectively. The spectra include the (unidentified) "background" peaks at 2340 and 2290 Å. The vibrational spacing in the $A0^-$ state was found to be 194 ± 6 cm^{-1}.

2. The $F1 \rightarrow X0^+$ fluorescence spectrum

Figure 8 shows traces of the fluorescence bands emitted in the $F1\rightarrow X0^+$ decay of the $v'=1$ and 0 levels. Both v' levels were excited from the $A0^+$ $v''=0$ state using 4258- and 4288-Å probe radiation, respectively. The

FIG. 8. LIF bands emitted from the $v'=1$ and 0 levels of the $F1$ state, excited from the $v''=0$, $A0^+$ state with 4258- and 4288-Å probe radiation. The trace includes structure due to background fluorescence.
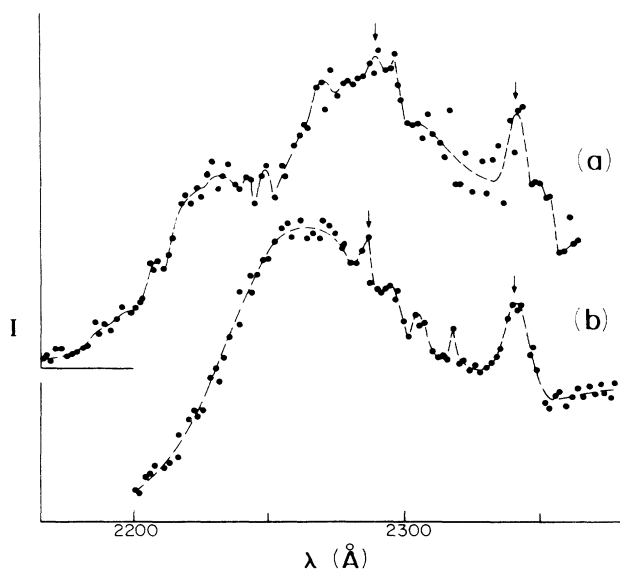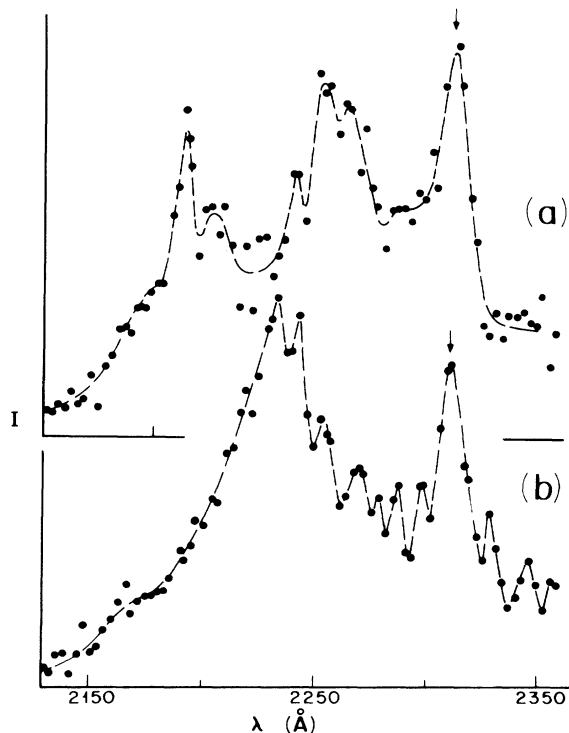

FIG. 7. LIF bands emitted from $v'=1$ and $v'=0$ levels of the $E1$ state, excited from the $v''=0$, $A0^-$ state with 4347- and 4372-Å probe radiation.
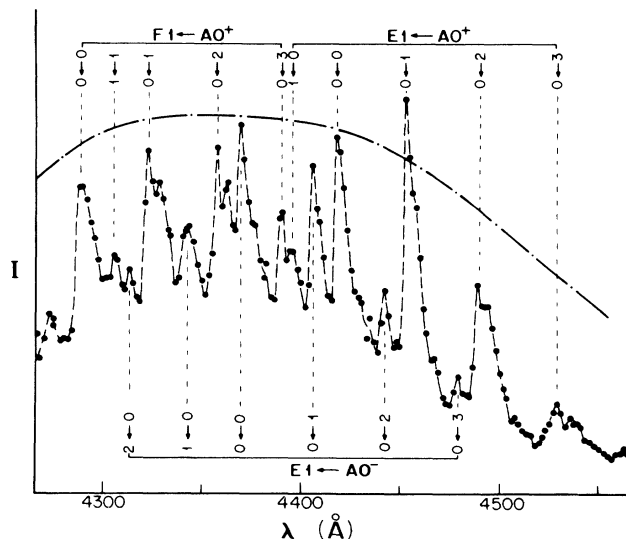

FIG. 9. A trace of the fluorescence-monitored excitation spectrum, showing the vibrational structures of the $F1\leftarrow A0^+$, $E1\leftarrow A0^-$, and $E1\leftarrow A0^+$ band systems. The $v'\leftarrow v''$ assignments are shown on the trace. The dashed line represents the dye-laser power curve.
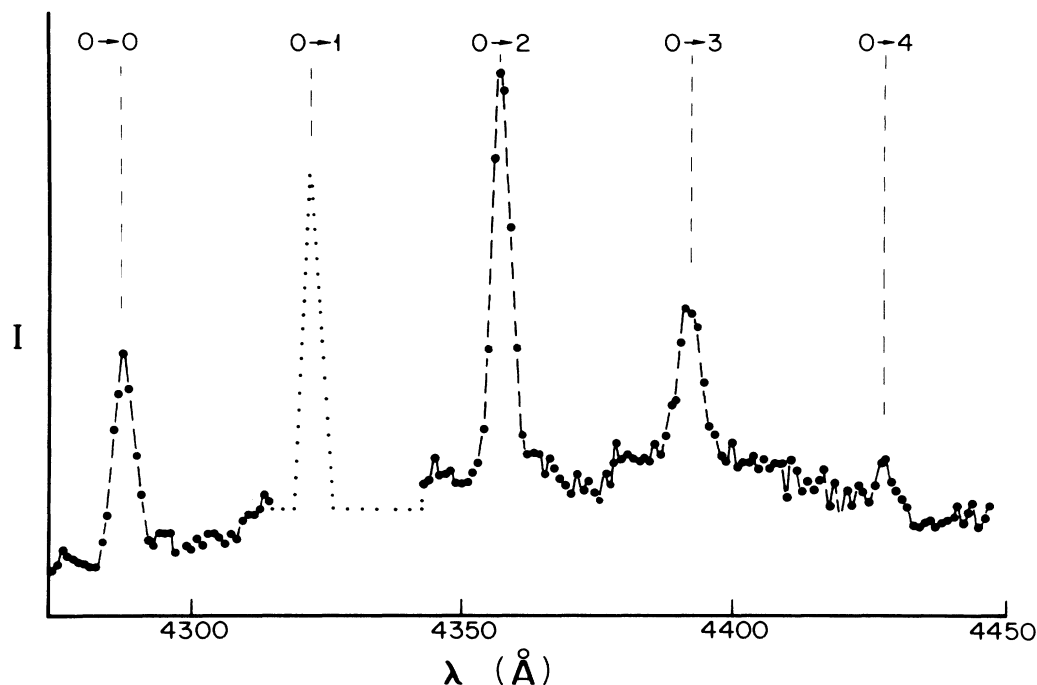
FIG. 10. A trace of the $F1 \to A0^+$ fluorescence band, showing $v'=0 \to v''$ assignments.

bands also include the background CID spectrum with the peak at 2340 Å quite prominent. It may be seen that the $v'=0$ component of the $F1$ state is centered at 2230 Å, and of the $E1$ state at 2260 Å. The effective lifetimes of the $E1$ and $F1$ states are estimated to be of the order of 1 ns as their decays appeared to follow the time evolution

of the probe-laser pulses. This might seem surprising since the $F1$ state is correlated with $Hg(6\,^1S)+Zn(5\,^3S)$, but it is found to have a strong admixture of other states, in particular $Hg(6\,^3P)+Zn(4\,^1S)$ near its minimum (see Fig. 1).

B. The excitation spectrum in the 4200–4500-Å region

Figure 9 shows the extensive and highly structured excitation spectrum recorded by scanning the probe laser over the range 4200–4550 Å while monitoring the fluorescence at 2250 Å. It consists of the vibrational structures of the $F1 \leftarrow A0^+$, $E1 \leftarrow A0^-$, and $E1 \leftarrow A0^+$ excitation bands which are identified in the trace. The $E1 \leftarrow A0^-$ and $E1 \leftarrow A0^+$, $v'=0 \leftarrow v''=0$ transitions give rise to components at 4372 and 4421 Å, respectively, and thus yield the energy separation of 253 ± 12 cm^{-1} between the $A0^+$ and $A0^-$ reservoir states. The peak corresponding to the $F1 \leftarrow A0^+$, $v'=0 \leftarrow v''=0$ transition is found at 4288 Å.

That all three bands include components arising from transitions between low v' and v'' levels leads to the conclusion that, in each case, the internuclear separations r_e in the upper and lower electronic states are nearly equal. The most intense components, at 4450 and 4496 Å, arise from the $E1 \leftarrow A0^+$, $v'=0 \leftarrow v''=1$, and $v'=0 \leftarrow v''=2$ transitions, respectively.

The excitation spectrum recorded by monitoring the fluorescence at 2340-, 2460, 2600-, or 2650-Å peaks in the background bound-continuous fluorescence spectrum had a structure quite different from that shown in Fig. 9, confirming our conclusions concerning the origin of the fluorescence peak at 2340 Å appearing in Figs. 6, 7, and 8.

TABLE I. Vibrational components of the $F1 \to A0^+$ fluorescence band; the measured λ (Å) are given in air, the $\tilde{v}$ (cm^{-1}) are stated *in vacuo.*

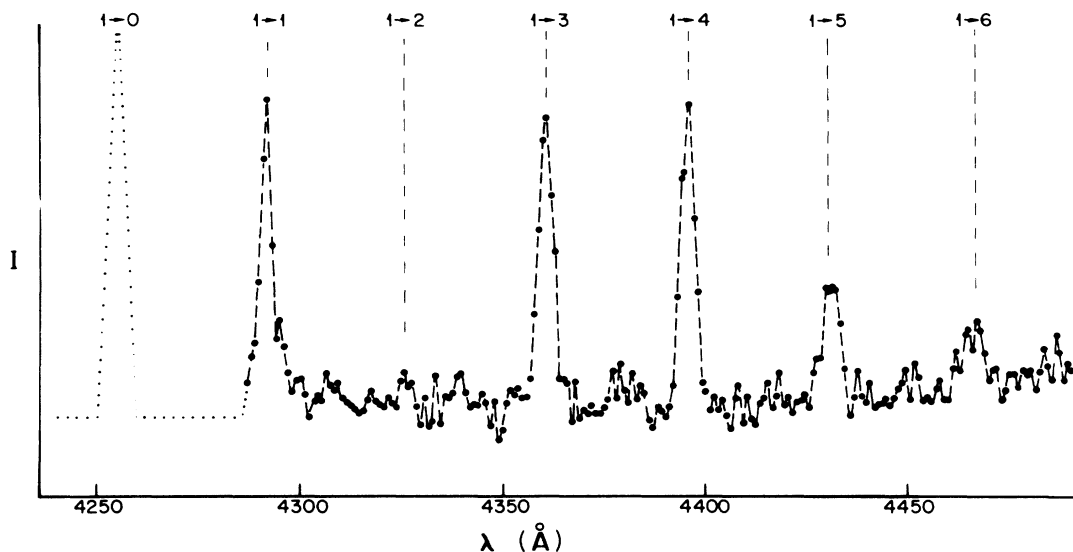| $v' \to v''$	λ (Å)	$\tilde{v}$ (cm^{-1})	$\Delta\tilde{v}$ (cm^{-1})
$0 \to 0$	4288 ± 1	$23\,314\pm5$	
			188
$0 \to 1$	4323 ± 1	$23\,126\pm5$	
			186
$0 \to 2$	4358 ± 1	$22\,940\pm5$	
			188
$0 \to 3$	4394 ± 2	$22\,752\pm10$	
			180
$0 \to 4$	4429 ± 3	$22\,572\pm15$	
$1 \to 0$	4258 ± 1	$23\,479\pm5$	
			186
$1 \to 1$	4292 ± 1	$23\,293\pm5$	
			189
$1 \to 2$	4327 ± 3	$23\,104\pm15$	
			180
$1 \to 3$	4361 ± 1	$22\,924\pm5$	
			182
$1 \to 4$	4396 ± 1	$22\,742\pm5$	
			185
$1 \to 5$	4432 ± 2	$22\,557\pm10$	
			177
$1 \to 6$	4467 ± 3	$22\,380\pm15$	

FIG. 11. A trace of the $F1 \rightarrow A0^+$ fluorescence band, showing $v'=1 \rightarrow v''$ assignments.

The shapes of the vibrational components of the excitation band can also provide an indication of the relative r_e values associated with the states involved in the transition. When the r_e values are similar, so are the rotational constants, and because of the rotational selection rules ($\Delta J = 0 \pm 1$), the rotational profile of a particular vibrational component will be relatively narrow. The larger the difference between the r_e values, the greater the broadening of the vibrational components. If the latter exhibit steep leading edges on the short-wavelength sides, this indicates that $r_e' > r_e''$. If the steep edges appear on the long-wavelength sides, then $r_e' < r_e''$.[7] The components of the v'' progressions associated with the $E1$ and $F1$ states seen in Fig. 9 are relatively narrow, exhibit steep leading edges, and are degraded towards longer wavelengths. These features which we ascribe to the effects of rotational structure, suggest that the r_e values
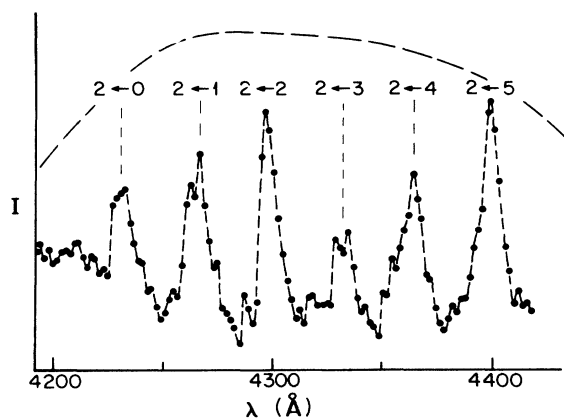

FIG. 12. A trace of the $F1 \leftarrow A0^+$ excitation spectrum, showing $v' \leftarrow v''$ assignments. The spectrum was monitored at 4435 Å, a fluorescence component arising from the $F1 \rightarrow A0^+$, $v'=2 \rightarrow v''=6$ decay.

of the $A0^-$ and $A0^+$ states on the one hand, the $F1$ and $E1$ states on the other, are nearly equal to one another with r_e' somewhat larger than r_e''. The separation of the $F1$ and $E1$ levels, determined from the excitation spectrum, agrees within experimental error with the spacing estimated from the bound-free spectra in Figs. 6 and 8.

C. The $F1 \rightarrow A0^+$ fluorescence spectrum

Figure 10 shows a trace of the $F1 \rightarrow A0^+$ (bound-bound) fluorescence band excited with the probe-laser wavelength 4323 Å which induced the $v'=0 \leftarrow v''=1$ transition. The structure of the spectrum represents a v'' progression with a spacing of 186 ± 6 cm^{-1} corresponding to ω_e for the $A0^+$ state. The $v'=0 \leftarrow v''=0$ component is at 4288 Å and thus the energy difference between the $v=0$ levels of the $F1$ and $A0^+$ states is $23\,314 \pm 12$ cm^{-1}. The vibrational components are identified on the trace and are listed in Table I; their relative intensities suggest a Gaussian distribution of FC factors, typical of a $v'=0$ emission. Figure 11 shows the corresponding fluorescence band arising from $v'=1 \rightarrow v''$ decays. The $v'=1$ level was populated by $v'=1 \leftarrow v''=0$ absorption, using the probe wavelength 4258 Å. The spectrum shows an intensity distribution typical for a $v'=1$ emission.

We also observed $F1 \leftarrow A0^+$ excitation spectra containing $v'=0 \leftarrow v''$ and $v'=1 \leftarrow v''$ progressions, which had structures identical to the fluorescence spectra in Figs. 10 and 11. Figure 12 shows a trace of the excitation spectrum arising from $v'=2 \leftarrow v''$ transitions; the spectrum was monitored at 4435 Å, the wavelength of a fluorescence component emitted in the $v'=2 \rightarrow v''=6$ transition.

VI. SUMMARY AND CONCLUSIONS

Pump and probe methods of laser spectroscopy were used to produce excitation and fluorescence spectra associated with the $E1$ and $F1$ states of the HgZn excimer,

TABLE II. Molecular constants obtained from the fluorescence and excitation spectra.

HgZn state	ΔE (cm^{-1})[a]	ω_e (cm^{-1})	$\omega_e x_e$	Δr_e (Å)[b]
$A0^-$	0	194 ± 6		0
$A0^+$	253 ± 12[c]	192 ± 6[c]	0.9 ± 0.2[c]	0
	0[e]	194 ± 4[d]	0.7 ± 0.2[d]	
$C0^+$	$17\,278\pm20$[d]	117 ± 4[d]	0.5 ± 0.2[d]	0.25 ± 0.01[d]
	14 000[e]			
$E1$	$22\,867\pm12$[c]	135 ± 10[c]		0.13 ± 0.01
	19 000[e]			
$F1$	$23\,567\pm12$[c]	167 ± 4[c]		0.13 ± 0.01
	21 000[e]			

[a]ΔE is the energy of the $v=0$ level relative to the $v=0$ level of the $A0^-$ state.
[b]Δr_e is determined relative to r_e ($A0^+$).
[c]This investigation.
[d]Reference 1.
[e]Estimated from the PE diagram.

which were populated by excitation from the $A0^-$ and $A0^+$ "reservoir" states. An analysis of the spectra carried out in conjunction with Hund's case-(c) PE curves obtained from a theoretical calculation led to assignments of the upper and lower electronic and vibrational states, yielded the respective vibrational constants, and provided information on the relative energies of the PE minima which are compared with the PE diagram. A simple modeling calculation[7] of the vibrational intensity distributions in the various spectra led to estimates of $\Delta r_e = r'_e - r''_e$, the differences between the internuclear separations in the upper and lower states involved in the transitions.

The results of these experiments taken in conjunction with the PE curves shown in Fig. 2 also lead to a reinterpretation of the previously reported spectra which were assigned to transitions between molecular states derived from Hund's case-(a) coupling,[1,2] a scheme which is not a good representation for the HgZn excimer and which has now been superseded.[2] Accordingly, we believe that the excitation spectrum observed in the region 5200–6650 Å

is due to transitions between vibrational levels of the $C0^+$(Hg ^1P+Zn ^1S) and $A0^+$(Hg ^1S+Zn ^3P) states, and the CID fluorescence spectrum in the 2400–2600-Å region arises from the $C0^+ \rightarrow X0^+$ decay. The various constants are summarized in Table II.

The assignments of the fluorescence and excitation spectra to the transitions between the $E1$, $F1$, $A0^-$, and $A0^+$ states as described above, are fully consistent with the calculated PE curves and selection rules, and with the just-completed analyses of additional HgZn spectra which will be fully described in a forthcoming publication.[6] The absence of other nominally allowed transitions is due to their small oscillator strengths.

*Permanent address: Laboratoire de Physico Chimie des Rayonnements, University of Paris XI, Orsay, France.
[1]J. Supronowicz, E. Hegazi, J. B. Atkinson, and L. Krause, Phys. Rev. A 37, 3818 (1988).
[2]J. Supronowicz, E. Hegazi, G. Chambaud, J. B. Atkinson, W. E. Baylis, and L. Krause, Phys. Rev. A 37 295 (1988).
[3]G. Herzberg, Spectra of Diatomic Molecules (Van Nostrand, New York, 1950).

[4]J. Niefer, J. Supronowicz, J. B. Atkinson, and L. Krause, Phys. Rev. A 34, 1137 (1986).
[5]W. Kedzierski, R. W. Berends, J. B. Atkinson, and L. Krause, J. Phys. E 21, 796 (1988).
[6]E. Hegazi, J. Supronowicz, J. B. Atkinson, and L. Krause (unpublished).
[7]R. J. Niefer, J. Supronowicz, J. B. Atkinson, and L. Krause, Phys. Rev. A 35, 4269 (1987).